# Numerical Prediction of Buckling in Ship Panel Structures

**Authors:**   **Gonghyun Jung** (V), **T.D. Huang** (V), **Pingsha Dong** (V), **Randal M. Dull** (V), **Christopher C. Conrardy** (V), **and Nancy C. Porter** (V)

## ABSTRACT

*Q-WELD™, a shell-element-based numerical module was used to effectively predict welding-induced distortions. The results of Q-WELD™ were validated by comparison with a series of physical test panels. Eigenvalue analyses were performed to evaluate the buckling propensity of each test panel with and without transient thermal tensioning.*

KEY WORDS: Buckling; Transient Thermal Tensioning; Panel Structure; Finite Element Analysis; Welding Sequence; Q-WELD™; Welding Distortion Mitigation; Weld Distortion Reduction.

## INTRODUCTION

Shipboard applications of lightweight structures have increased over recent years in both military and commercial vessels. Buckling distortion of complex lightweight structures has emerged as a major obstacle to the cost-effective fabrication for shipbuilders. High-strength thin steel material reduces topside weight, enhances mission capability, and improves performance and vessel stability, but greatly increases the propensity of structural buckling distortion. Transient thermal tensioning (TTT) is a particularly promising technique that minimizes heat-induced buckling distortion in a relatively simple process.

Without significant loss of productivity, TTT is applied concurrently to, but some distance away from, the existing welding torch during fabrication. TTT has faced the challenge in more complex panel structures reinforced by long slender stiffeners along with numerous cutouts and inserts. This geometric complexity yielded a more complicated buckling behavior, which drives the need to develop a more fine-tuned finite element (FE) model to determine critical parameters and heating patterns for the thermal tensioning process.

During ship panel fabrication, undesirable distortions induced by welding, such as excessive angular distortion, longitudinal bending (*i.e.,* bowing), transverse shrinkage, and buckling (*i.e.,* waviness of free edges and skin plate between stiffeners), increase the production cost to repair the panels before they can progress to the next fabrication stage. The general in-service structural performance is decreased due to secondary stresses induced by assembling misaligned parts, and reduced buckling resistance caused by initial geometric imperfections.

In the application of lightweight panel structures, the cost of materials (*i.e.,* base material and filler metal) is reduced by using thin and high strength materials. As a result, one of critical issues is the higher buckling propensity of thin plates under external loads and/or compressive residual stress induced by welding. Considering the influence of initial imperfections on buckling resistance, buckling should be minimized or eliminated during welding (Smith 1977, Carlson 1980, Horne 1976 and 1977). Otherwise, the buckled panel should be analyzed to determine if it satisfies the design requirement.

Therefore at the design stage, a buckling analysis should be carried out considering not only external load, but also compressive residual stress induced by welding. However, it is not practical for welding and structural designers to consider both external and welding driving forces to find the optimized structure dimensions and welding parameters. Furthermore, if the panel were inherently weak within the design welding window, its thickness should be increased, which may reduce the benefit of the lightweight panel. In these cases, applying distortion mitigation techniques is the preferred method to effectively increase buckling resistance without changing panel dimensions and welding parameters. Distortion mitigation techniques include mechanical restraining, pre-straining, thermal treatments, etc.

Some distortion mitigation techniques that have been investigated and determined to be effective in the control of buckling are reverse arching (Huang 2005), static/transient thermal tensioning (Michaleris 1997; Huang 2005), low-stress and non-distortion (Guan 1988). Regardless of the type of techniques used to control of buckling, these techniques may be categorized into two groups; reducing the buckling driving forces by reducing the compressive longitudinal plastic strain (*e.g.,* reverse arching), or increasing the buckling resistance of the structure (*e.g.,* static/TTT).

With a recent major initiative funded by the U.S. Navy, Northrop Grumman Ship Systems (NGSS) has undertaken a comprehensive assessment of lightweight structure fabrication technology. NGSS has teamed with Edison Welding Institute (EWI), Battelle Memorial Institute, The University of New Orleans, The University of Michigan, and The Pennsylvania State University's Applied Research Laboratory (ARL) on this initiative to develop a preferred manufacturing plan for lightweight ship structures. Through the collaborative research works, significant progresses have been achieved in the development of distortion control techniques (Huang 2004). TTT, reverse arching, stiffener welding assembly sequencing, and other preferred manufacturing techniques were developed to reduce distortion and eliminate the high rework costs associated with correcting welding distortion.

This study is focused on the application of TTT in Navy ship panel structures. TTT is a promising technique known for minimizing buckling in relatively simple panel structures without significant loss of productivity and because TTT is applied concurrently with the welding process, it does not require major changes to existing welding systems. In the application of TTT, it is important to determine the proper parameters, such as the location of the heat line, heat input, etc. This can be accomplished through small- and/or large-scale testing and

| Report Documentation Page | | Form Approved OMB No. 0704-0188 |
|---|---|---|

Public reporting burden for the collection of information is estimated to average 1 hour per response, including the time for reviewing instructions, searching existing data sources, gathering and maintaining the data needed, and completing and reviewing the collection of information. Send comments regarding this burden estimate or any other aspect of this collection of information, including suggestions for reducing this burden, to Washington Headquarters Services, Directorate for Information Operations and Reports, 1215 Jefferson Davis Highway, Suite 1204, Arlington VA 22202-4302. Respondents should be aware that notwithstanding any other provision of law, no person shall be subject to a penalty for failing to comply with a collection of information if it does not display a currently valid OMB control number.

| 1. REPORT DATE **2006** | 2. REPORT TYPE | 3. DATES COVERED **00-00-2006 to 00-00-2006** |
|---|---|---|
| 4. TITLE AND SUBTITLE **Numerical Prediction of Buckling in Ship Panel Structures** | | 5a. CONTRACT NUMBER |
| | | 5b. GRANT NUMBER |
| | | 5c. PROGRAM ELEMENT NUMBER |
| 6. AUTHOR(S) | | 5d. PROJECT NUMBER |
| | | 5e. TASK NUMBER |
| | | 5f. WORK UNIT NUMBER |
| 7. PERFORMING ORGANIZATION NAME(S) AND ADDRESS(ES) **Office of Naval Research -Navy Mantech,Center for Naval Shipbuilding Technology (CNST) ,5300 International Blvd,Charleston,SC,29418** | | 8. PERFORMING ORGANIZATION REPORT NUMBER |
| 9. SPONSORING/MONITORING AGENCY NAME(S) AND ADDRESS(ES) | | 10. SPONSOR/MONITOR'S ACRONYM(S) |
| | | 11. SPONSOR/MONITOR'S REPORT NUMBER(S) |
| 12. DISTRIBUTION/AVAILABILITY STATEMENT **Approved for public release; distribution unlimited** | | |
| 13. SUPPLEMENTARY NOTES | | |
| 14. ABSTRACT **see report** | | |
| 15. SUBJECT TERMS | | |

| 16. SECURITY CLASSIFICATION OF: | | | 17. LIMITATION OF ABSTRACT **Same as Report (SAR)** | 18. NUMBER OF PAGES **9** | 19a. NAME OF RESPONSIBLE PERSON |
|---|---|---|---|---|---|
| a. REPORT **unclassified** | b. ABSTRACT **unclassified** | c. THIS PAGE **unclassified** | | | |

**Standard Form 298 (Rev. 8-98)**
Prescribed by ANSI Std Z39-18

analytical/numerical predictions, in order to avoid an undesirable degradation of structural and material performance.

The small-scale tests can be used to find basic TTT parameters, such as heat input (*e.g.,* travel speed, gas flow rate, type of gas, etc.) to maintain the critical maximum peak temperature and to perform sensitivity studies to determine the best location for heat lines with respect to buckling resistance. Buckling is associated with the driving force for distortion (*i.e.,* the shrinkage force induced by welding) and with the dimensions of structures. Small-scale tests do not provide sufficient information to investigate buckling propensity of the large-scale panel structures, but it is not practical or necessary to test large-scale panel structures to determine optimal TTT parameters. Numerical models incorporating not only proper buckling driving forces, but dimensions and boundary conditions of full-scale panel structures can be developed to determine optimal TTT parameters.

Several numerical models have been developed and used in buckling analysis of ship panel structures; shrinkage-force-based buckling analysis and thermoplasticity-based buckling analysis (Huang 2003). For complex panel structures with inserts, cutouts, and stiffeners, the development of new numerical models was recommended to incorporate various TTT conditions. In order to perform parametric studies with the various TTT conditions, a new numerical model should provide a fast solution without losing significant accuracy.

A new numerical model should consider the precise buckling driving force (*i.e.,* longitudinal plastic strain) resided in various weld joints and the proper structural stiffness and boundary conditions. Plasticity-based distortion analysis (PDA) was developed which enables mapping of plastic strains into a finite element (FE) model using the equivalent thermal strains (Jung 2003). As a result, EWI developed A shell-element-based numerical module (Q-WELD$^{TM}$) which maps plastic strains into a FE model.

The validity of Q-WELD™ to conduct buckling analysis was evaluated via comparison with the results of a series of physical test panels.

## Introduction of Q-WELD™

Q-WELD$^{TM}$ was developed at EWI to predict welding distortions of large-scale welded structures. Q-WELD$^{TM}$ is an ABAQUS User-Subroutine which enables to map the distortion sources (plastic strains) into shell element-based FE models. Theoretical background of Q-WELD$^{TM}$ development is based on a Ph.D. dissertation (Jung 2003) and subsequent publications (Jung 2003, Jung 2005; Jung 2004a, Jung 2004b; Jung 2005)

Q-WELD$^{TM}$ is applicable in the prediction of welding or heat treating-induced distortions including out-of plane distortion (*i.e.,* angular distortion), longitudinal bending, transverse shrinkage, and buckling. The distortion prediction can be done through most of ABAQUS solution capabilities including material and geometry nonlinearities, such as linear elastic analysis, large deformation elastic-plastic analysis, eigenvalue analysis, etc.

Q-WELD$^{TM}$ is not a stand-alone program for predicting welding distortion like thermal-elastic-plastic analysis (TEPA). The inputs of Q-WELD$^{TM}$ are angular distortion, magnitude of maximum transverse and longitudinal plastic strains, and the size of plastic zone which depend on welding process, welding parameters, materials, and joint configuration. These inputs should be obtained from a well-evaluated

thermal-elastic-plastic analysis and/or welding tests for the specified welding conditions.

When the structure has repetitive joints, the application of Q-WELD$^{TM}$ is more beneficial. For example, when a panel consists of repetitive joints with the same joint configuration and welding conditions, the input of Q-WELD$^{TM}$ can be prepared by running a TEPA and/or welding tests on only one representative welding joint. The distortion induced by the entire welding can then be predicted by mapping the distortion sources through Q-WELD$^{TM}$. The problem can be defined elastically or elastic-plastically depending on the degree of restraint between adjacent welded structural members (Jung, 2005); however, Q-WELD™ does not consider the change of plastic strains due to temperature interaction between adjacent heat sources.

## Buckling Analysis Using Q-WELD™

The instability of structures under compressive loadings can be evaluated by eigenvalue analysis and/or large deformation analysis. In simple cases, linear eigenvalue analysis is sufficient for design evaluation; but in other unstable analyses the instabilities are local (*e.g.*, surface wrinkling, material instability or local buckling), large deformation analysis with stabilizing instantaneous buckling or collapse can be used (ABAQUS 2004).

In this study, eigenvalue analysis was adopted in the design evaluation for panels and in the welding sequence analysis. Elastic-large deformation analysis was carried out in order to consider consequently updated geometric configurations while each weld joints were constructed one by one.

Fig. 1 shows the buckling analysis procedure. It is critical to obtain the proper plastic strain information for the given material, geometry, and welding procedure.
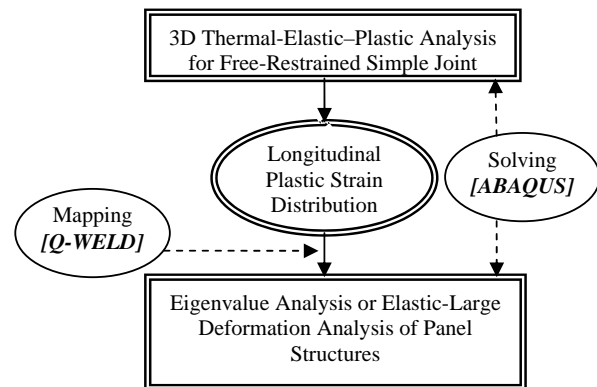


**Fig. 1.   Buckling Analysis Procedure Using Q-Weld™**

***3D TEPA of Free-Restrained Simple Joint.***   A 609.6-mm long by 1,219.2-mm wide panel was fabricated with one stiffener (101.6 mm × 101.6 mm, 5 mm thick T-beam). Both fillet welds were made simultaneously by flux cored arc welding (FCAW) with two weld guns (lead and trail) running with an offset distance of 4-in. (101.6-mm). Travel speed was 9.74 mm/s, and heat input for leading and trail welding arcs was 0.63 kJ/mm, and 0.47 kJ/mm, respectively. The material was ABS Grade AH36 steel, with typical thermal-mechanical properties shown in Fig. 2.
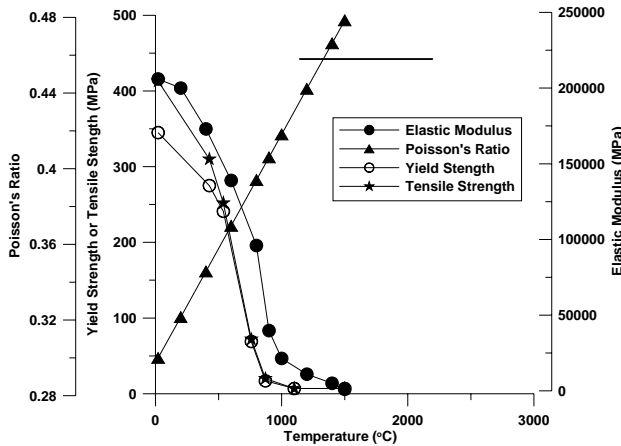
Fig. 2.    Mechanical Properties of AH36



Fig. 3.    Distribution of Longitudinal Plastic Strains on Flange Plate

From the free-restrained simple joint, the longitudinal plastic strain distributions on the top and bottom surface of the flange plate were obtained as shown in Fig.3.    For this thin panel, the longitudinal plastic strain distributes uniformly through thickness.    The size of the plastic zone is about 76-mm and the minimum longitudinal plastic strain is about -0.002.

Fig. 4 shows the associated longitudinal residual stress.    Tensile stress induced by the compressive longitudinal plastic strain presents near the weld joint, and compressive stress present at the region away from the weld joint.    The compressive longitudinal stress is driven by satisfying force and moment equilibrium, causing buckling if the resultant shrinkage force exceeds the panel's buckling resistance.    The maximum tensile stress is 366 MPa and minimum compressive stress is approximately 84 MPa.

This longitudinal plastic strain was used as the buckling driving force induced by welding, and was mapped into shell-element-based FE model with Q-WELD™.

***Eigenvalue and Elastic-Large Deformation Analysis Using Q-WELD™.***    The obtained plastic strains from 3D TEPA were mapped into shell element-based FE models using Q-WELD™.    In this study, angular distortion induced by the gradient of transverse plastic strain and in-plane (cross section of weld) shear plastic strain was not considered except elastic-large deformation analysis for 0.6-m by 1.2-m panel.

It was assumed that the panels were initially flat in eigenvalue analysis, but in the elastic-large deformation analysis, the deformed shapes as initial perturbation associated with specific eigenmode (0.6-m by 1.2-m panel) or self-weight (4.9-m by 6.1-m panel for welding sequence analysis) was considered when both final magnitude and shape of deformation were concerned.

Note that plastic strain distribution induced by TTT was assumed to have a 40-mm plastic zone width and half the magnitude of longitudinal plastic strain due to welding ( = -0.001) without running 3D EPA.
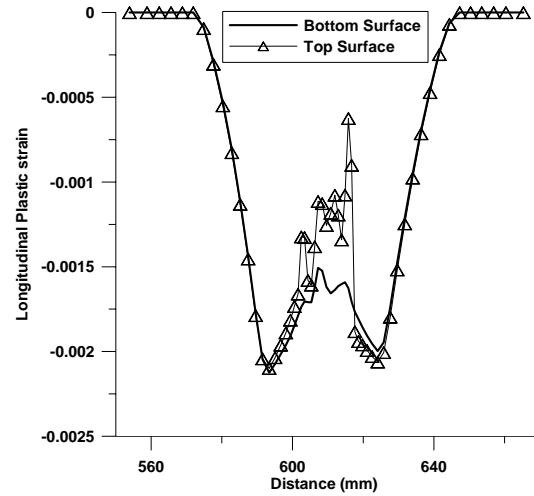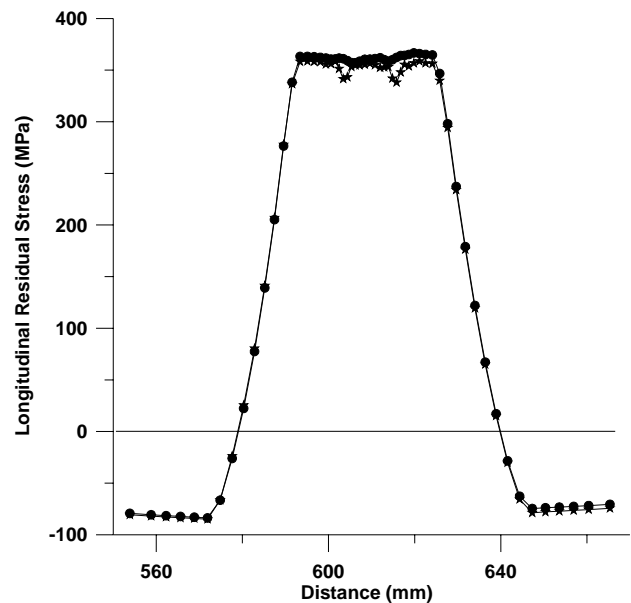


Fig. 4.    Distribution of Longitudinal Residual Stress on Flange Plate

## Case Studies

The following panels were tested and simulated to evaluate the validity of the Q-WELD™ application to assess buckling propensity with and without TTT.

- 0.6-m by 1.2-m panel with single stiffener
- 4.9-m by 6.1-m NGSS panel design #1 with 8 stiffeners

- 4.9-m by 6.1-m NGSS panel design #3 with 8 stiffeners and insert plate (10-mm thick)

Since this study focused on investigating the relative buckling propensity with and without TTT, the same plastic strain was applied in all case studies: a 40-mm wide plastic zone and -0.001 maximum longitudinal plastic strain. The correct plastic strain distribution for TTT can be obtained by 2D or 3D TEPA.

*Case Study 1: 0.6 m by 1.2 m Panel.* In this case study, the effect of heat line location of TTT on buckling propensity was investigated using eignevalue analysis and elastic-large deformation analysis. All components of plastic strains were considered in the elastic large deformation analysis.

The material was A36, and heat input for welding and TTT were similar to that described in the previous section. It was assumed that shrinkage forces are similar in A36 and AH36.

Four trials was made: without TTT (Case 1-Trial 1), with TTT at 15.2-cm away from weld (Case 1-Trial 2), with TTT at 20.3-cm away from weld (Case 1-Trial 3), and with TTT at 25.4-cm away from weld (Case 1-Trial 4).

Fig. 5 shows the first four calculated eigenmodes and eigenvalues for the case without TTT. The twisted deformation for this panel is expected after welding, because the eigenvalue of this mode (the first mode) is less than 1.
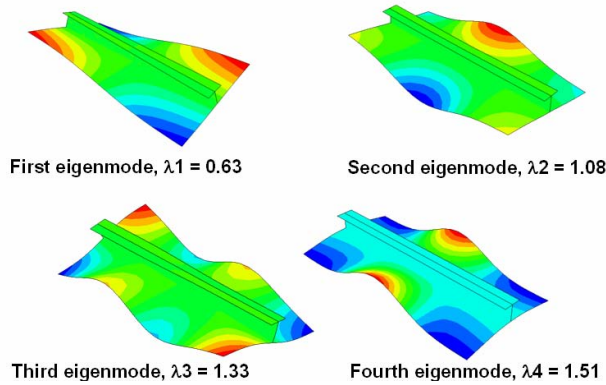


First eigenmode, $\lambda 1 = 0.63$        Second eigenmode, $\lambda 2 = 1.08$

Third eigenmode, $\lambda 3 = 1.33$        Fourth eigenmode, $\lambda 4 = 1.51$

**Fig. 5.    First 4 Eigenmodes and Eigenvalues for Case 1-Trial 1 (without TTT)**

Fig. 6 compares the measured and predicted out-of plane distortion for all trials. Q-WELD$^{TM}$ predicted well-matched distortion patterns and relative magnitude of out-of plane distortions compared to tests. For this small panel, it is shown that global buckling, twisting mode, is dominant if buckling occurs.

Both test and simulation result in the same effect of heat line locations on buckling propensity. TTT at 15.2-cm away from weld induces more buckling than without TTT. Trial 2 had smaller eigenvalue (from eigenvalue analysis) and larger out-of plane distortion (from elastic-large deformation analysis) than Trial 1 [eigenvalues = 0.58 < 0.63 and out-of plane distortion = 1.1-in (27.9-mm) > 0.9-in (22.9-mm)]. The buckling resistance starts to increase with TTT at 20.3-cm and then eliminates buckling with TTT at 25.4-cm, which is 5.1-cm from the free edge.

From this case study, the importance of the heat line location was addressed; TTT should not be close to welding. Initially, it was understood that applying TTT away from the weld was done in order to reduce the interaction between welding and TTT, so that the maximum peak temperature (about 370 °C) could be maintained to avoid material degradation and the change of characteristic plastic strain distribution of welding and TTT.
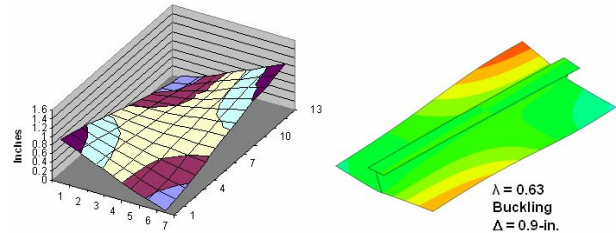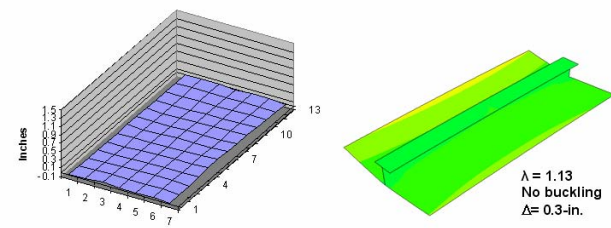


**(a) Case 1-Trial 1 (Without TTT)**
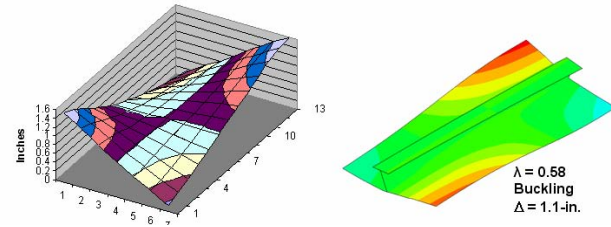


**(b) Case 1-Trial 2 (With TTT at 15.2-cm from Weld)**
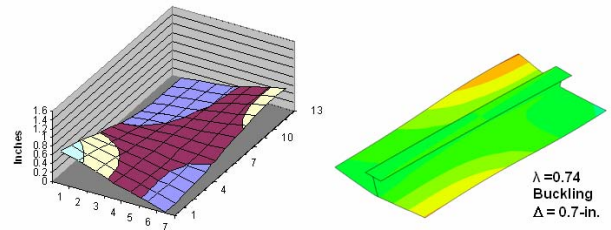


**(c) Case 1-Trial 3 (With TTT at 20.3-cm from Weld)**



**(d) Case 1-Trial 4 (With TTT at 25.4-cm from Weld)**

**Fig. 6.    Comparison of Measured and Predicted Deformation using Eigenvalue and Elastic Large Deformation Analyses**

From the Q-WELD™, results , it was revealed that the effectiveness of TTT gradually decreases as TTT gets closer to welding even though the interaction of welding and TTT on plastic strain distribution was not considered. Fig. 7 shows the variation of maximum principal stress distribution due to TTT. The tensioning region at the free edges becomes more pronounced as the distance between welding and TTT increases. Therefore, lateral tensioning induced by TTT (on the free edges) may be one of the sources increasing the buckling resistance of the panel.
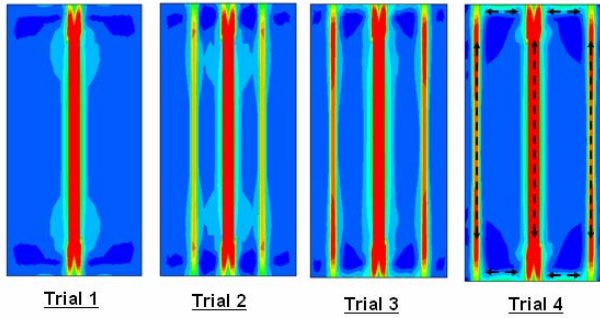


**Fig. 7.   Maximum Principal Stress Distributions**

***Case Study 2: 4.9 m by 6.1 m Panel Design #1.***   Case Study 2 was conducted with NGSS Panel Design #1, which consisted of a 5-mm thick, 4.9-m by 6.1-m plate (DH-36) with eight WT 100 x 7.5 stiffeners (AH-36) welded as shown in Fig. 8. Nominal welding heat input was 0.63 kJ/mm. for the lead torch and 0.55 kJ/in. for the trail torch.
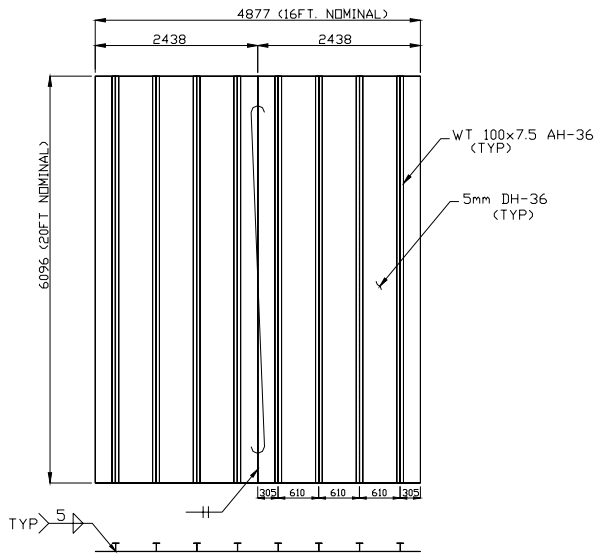


**Fig. 8.   NGSS Panel Design #1**

For NGSS Panel Design #1 without TTT, Fig.9 shows the first five eigenmodes and corresponding eigenvalues predicted from buckling analysis with Q-WELD™™. The first two eigenmodes are associated with global buckling. Eigenmodes 3 through 5 have waviness on the free edge. The first five eigenvalues were less than 1, so buckling was

expected in NGSS Panel Design #1 without TTT and its deformation could be the combination of global and local buckled shapes.

Fig. 10 shows results of LIDAR scanning and Q-WELD™ analysis (third eigenmode) of NGSS Panel Design #1 without TTT. The Q-WELD™ analysis predicted buckling with a similar deformation pattern as observed in the LIDAR scan (*i.e.,* wavy deformation on the free edges).
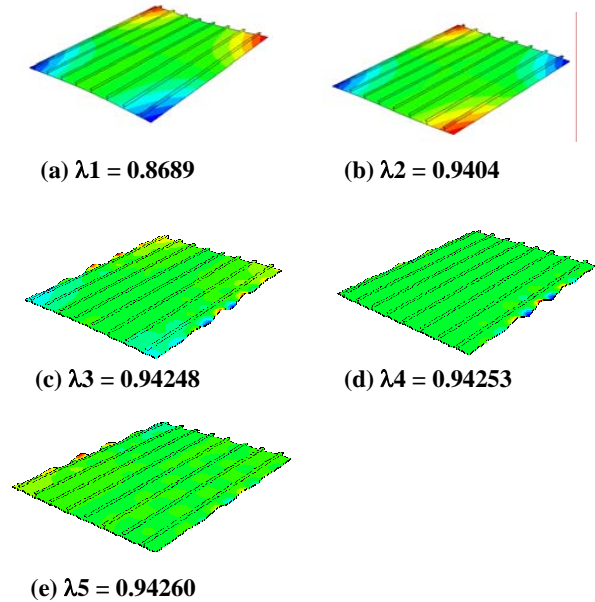


**(a) λ1 = 0.8689**        **(b) λ2 = 0.9404**

**(c) λ3 = 0.94248**       **(d) λ4 = 0.94253**

**(e) λ5 = 0.94260**

**Fig. 9.   First 5 Eigenmodes and Eigenvalues for NGSS Panel Design #1 without TTT**



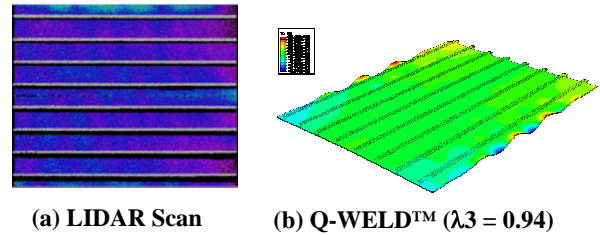**(a) LIDAR Scan**        **(b) Q-WELD™ (λ3 = 0.94)**

**Fig. 10.   Measured and Predicted Buckling Distortion for NGSS Panel Design #1 without TTT**

For NGSS Panel Design #1, the locations of the TTT heat lines are shown in Fig. 11 which represents the applied longitudinal plastic strains via Q-WELD™; two TTT on free edges (5.08-cm away from the edge) and six TTT lines between the stiffeners. The nominal TTT heat input used in the test was 0.47 kJ/mm.
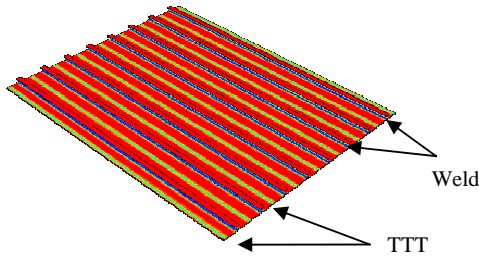
**Fig. 11.    Applied Longitudinal Plastic Strains via Q-WELD™ for NGSS Panel Design #1**

For NGSS Panel Design #1 with TTT, Fig. 12 shows the first three eigenmodes and corresponding eigenvalues predicted from buckling analysis.    The first two modes are associated with global buckling and their corresponding eigenvalues are negative.    This means that buckling can occur under reverse loading which is not expected to occur (ABAQUS, 2004).
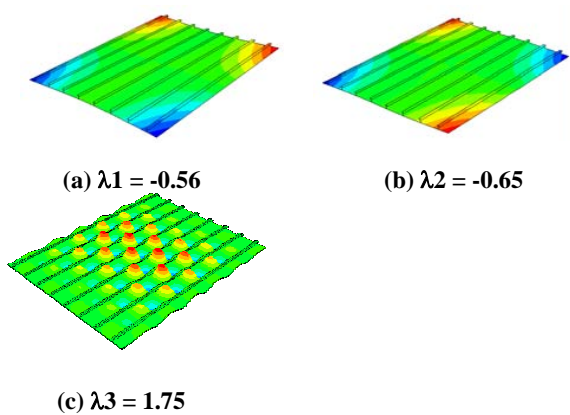


**(a) $\lambda 1 = -0.56$**            **(b) $\lambda 2 = -0.65$**



**(c) $\lambda 3 = 1.75$**

**Fig. 12.    First 3 Eigenmodes and Eigenvalues for NGSS Panel Design #1 with TTT**

Even though complicated deformation including wavy free edges is shown in the third mode, its eigenvalue is much greater than 1, which means no buckling is expected for NGSS Panel Design #1 with TTT.
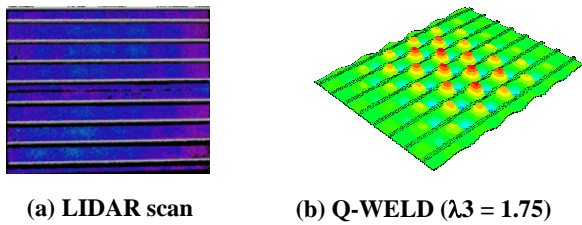
This is agreement with LIDAR scan shown in Fig. 13.



**(a) LIDAR scan**            **(b) Q-WELD ($\lambda 3 = 1.75$)**

**Fig. 13.    Measured and Predicted Buckling Distortion for NGSS Panel Design #1 with TTT**

The comparison of LIDAR scans and Q-WELD™ buckling analysis show good agreement for the Panel #1 design both with and without TTT.

*Case Study 3: 4.9 m by 6.1 m Panel Design #3.*    Case Study 3 was conducted with the NGSS Panel Design #3, which consisted of a welded base plate that was nominally 4.9-m. by 6.1-m. with 5-mm and 10-mm thick plate (DH-36), eight WT 100 x 7.5 stiffeners (AH-36), and a 10-mm thick insert that forms the welded assembly shown in Fig. 14.    Nominal welding heat input was 0.63 kJ/mm. for the lead torch and 0.55 kJ/in. for the trail torch.

For NGSS Panel Design #3 without TTT, Fig. 15 shows the first nine eigenmodes and corresponding eigenvalues predicted from Q-WELD™ buckling analysis.    The first mode is associated with global buckling. Waviness of free edges is shown starting in the second eigenmode.    In terms of resistance to local buckling, the edge near the insert (eigenvalue range of 0.74 to 0.85) is weaker than the other edge (eigenvalue range of 0.92 to 0.94).    Q-WELD™ buckling analysis predicted that both free edges would contain wavy deformation with more severe deformation occurring on the edge near the insert.
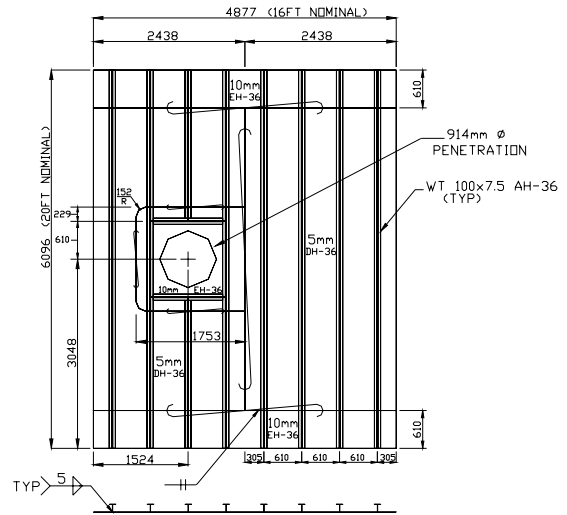


**Fig. 14.    NGSS Panel Design #3**



**(a) $\lambda 1 = 0.45$**            **(b) $\lambda 2 = 0.74$**            **(c) $\lambda 3 = 0.75$**

**(a) $\lambda 4 = 0.84$**            **(b) $\lambda 5 = 0.85$**            **(c) $\lambda 6 = 0.91$**

**(a) $\lambda 7 = 0.92$**            **(b) $\lambda 8 = 0.93$**            **(c) $\lambda 9 = 0.94$**
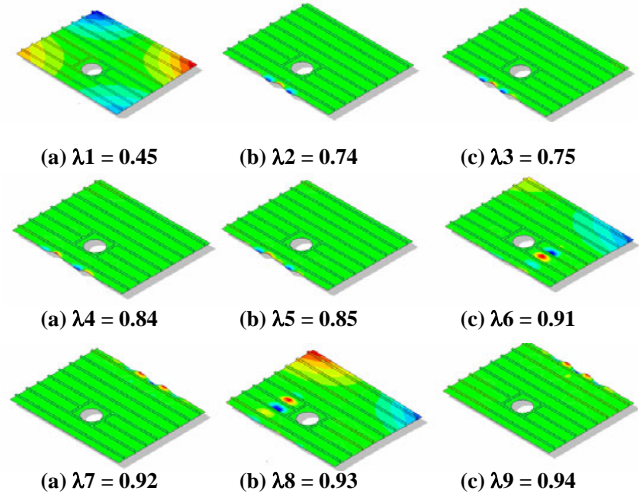
**Fig. 15.    First 9 Eigenmodes and Eigenvalues for NGSS Panel Design #3 without TTT**

Fig. 16 shows the LIDAR scan and Q-WELD™ results of NGSS Panel Design #3 without TTT. Even though these results are from the cases with different fillet sizes (LIDAR = 4-mm and Q-WELD™ = 5-mm), the Q-WELD™ prediction was in good agreement with the LIDAR scan, as Q-WELD™ indicated that the two free edges were potentially weak regions. Theoretically, if Q-WELD™ buckling analysis were performed with a 4-mm fillet size, each eigenvalue would increase, but the corresponding eigenmodes would be similar to with a 5-mm fillet size. The amount of buckling difference between cases with 4- and 5-mm fillet sizes could be studied by comparing longitudinal plastic strain distribution patterns obtained from thermal-elastic-plastic analysis
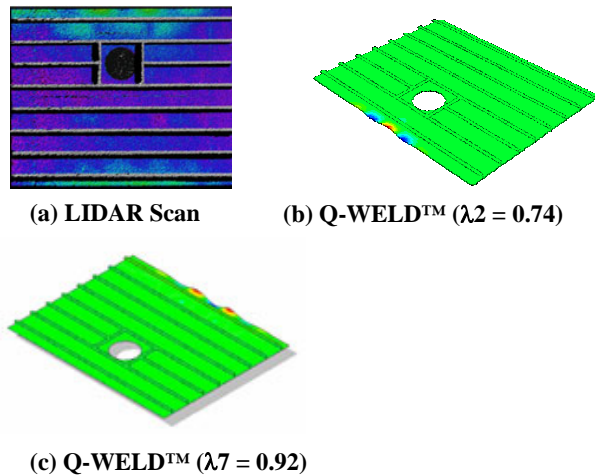


**(a) LIDAR Scan**          **(b) Q-WELD™ (λ2 = 0.74)**



**(c) Q-WELD™ (λ7 = 0.92)**

**Fig. 16.    Measured and Predicted Buckling Distortion for NGSS Panel Design #3 without TTT**

For NGSS Panel Design #3, the locations of the TTT heat lines are shown in Fig. 17. For the physical tests, two heat lines were applied 5.08-cm apart between the stiffeners that cross the insert. For the Q-WELD™ model, these two narrow heat lines were replaced with one wide heat line to simplify the model.
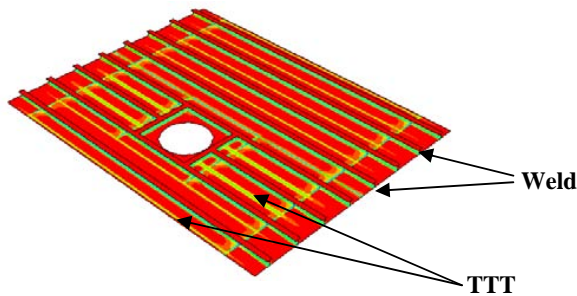


**Fig. 17.    Applied Longitudinal Plastic Strains vai Q-WELD™ for NGSS Panel Design #3**

For this case study, Q-WELD™ buckling analysis used the same plastic strains as the previous analyses (*i.e.*, 5-mm fillet size). For NGSS Panel Design #3 with TTT, Fig. 18 shows the first two eigenmodes and corresponding eigenvalues predicted from the Q-WELD™ buckling analysis. The first mode is associated with global

buckling; local buckling is shown in the second eigenmode. The eigenvalues associated with the global and local buckling were greater than 1, which means no buckling is predicted.
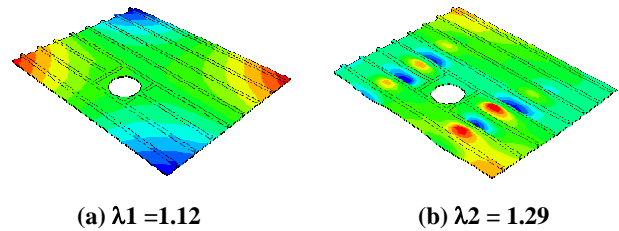


**(a) λ1 =1.12**          **(b) λ2 = 1.29**

**Fig. 18.    First 2 Eigenmodes and Eigenvalues for NGSS Panel #3 with TTT**

Fig. 19 shows results of the LIDAR scan and Q-WELD™ (second eigenmode) of NGSS Panel Design #3 with TTT. Q-WELD™ analysis predicted no buckling. Minor buckling was observed along the edge near the insert in the LIDAR scan.
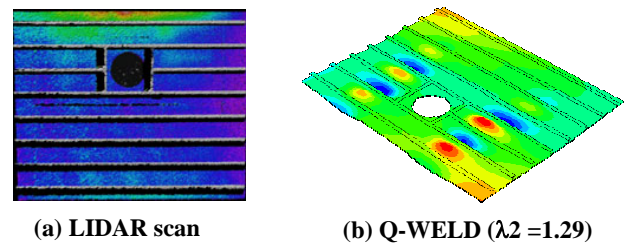


**(a) LIDAR scan**          **(b) Q-WELD (λ2 =1.29)**

**Fig. 19.    Measured and Predicted Buckling Distortion for NGSS Panel Design #3 with TTT**

The comparison of LIDAR scans and Q-WELD™ shows that TTT does effectively increase buckling resistance for NGSS Panel Design #3. For the trial without TTT, both LIDAR scan and Q-WELD™ show good agreement. Q-WELD™ predicted buckling would occur. For the trial with TTT, the Q-WELD™ predicted no buckling. However, the test with TTT did not eliminate buckling even though 3-mm fillets were deposited. This implies that an eigenvalue of 1.29 may not be sufficient to resist buckling, because of the initial imperfections due to variations in cutting, fitting, and welding of the insert, and other factors. This may also represent the important of distortion control planning for other processes (cutting, fitting, and insert welding, etc.) to reduce buckling propensity during welding stiffeners.

***Case Study 4: Welding Sequence Analysis for 4.9 m by 6.1 m Panel Design #1.*** For NGSS Panel Design #1, EWI used Q-WELD™ to predict the resultant distortion of the following two stiffener welding sequences with and without TTT.

- Edge-to-Center

- Center-to-Edge

A half-symmetric FE model was developed. The fabrication welding procedure was considered in this analysis; each stiffener was pressed down before and during welding, and then the restraint was released after welding. In order to consider local buckling behavior,

subsequently updated geometric configurations, and restraints, elastic-large deformation analysis was performed with initial perturbation induced by self-weight. It was assumed that the panel was supported by a 609.6-mm spaced foundation as shown in Fig. 20.
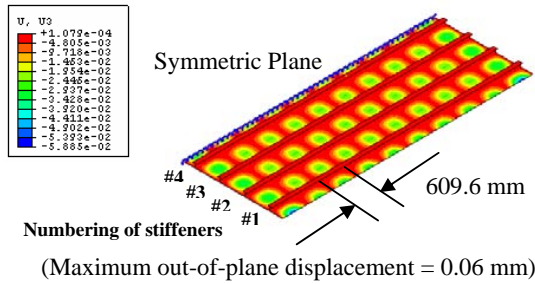


(Maximum out-of-plane displacement = 0.06 mm)

**Fig. 20. Initial Deformation Induced by Self-Weight for NGSS Panel Design #1**

Note that the maximum longitudinal plastic strain of welding and TTT used in these analyses was 25% higher than the previous analyses in order to make deformation more apparent. TTT was not applied.

For the welding sequence from the edge to the center; stiffener welding was conducted in the order of #1, #2, #3, and #4. Fig. 21 shows the deformed shapes after releasing restraints that were applied before and during welding. Buckling occurs at the free edge right after welding stiffener #1; the panel became more unstable with subsequent welding.
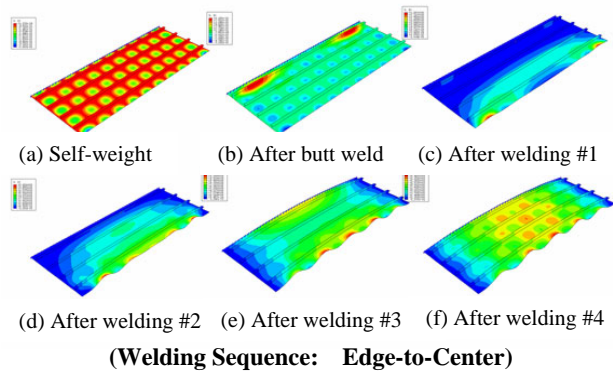


(a) Self-weight    (b) After butt weld    (c) After welding #1

(d) After welding #2    (e) After welding #3    (f) After welding #4

**(Welding Sequence: Edge-to-Center)**

**Fig. 21 Deformed shapes after welding each stiffener**

For the welding sequence from the center to the edge; welding stiffeners was conducted in the order of #4, #3, #2, and #1. Fig. 22 shows the deformed shapes after releasing restraints. No significant buckling occurred at the free edge until after welding stiffener #1 (the last stiffener welded).

Q-WELD™ predicted the edge-to-center sequence induced more severe buckling deformation than the center-to-edge sequence. For the edge to center sequence, welding started the weak region (free edge) where buckling occurred after welding (See, Fig. 21-c). This buckled configuration increases the buckling propensity for the subsequent welding. Therefore, buckling is getting more and more while welding is moving into the center from the edge. On the other hands, for the center to edge sequence, welding started from the region with the high

buckling resistance, which reduced the initial imperfection induced by the prior welding (See, Fig. 22-c) and the final buckling distortion.
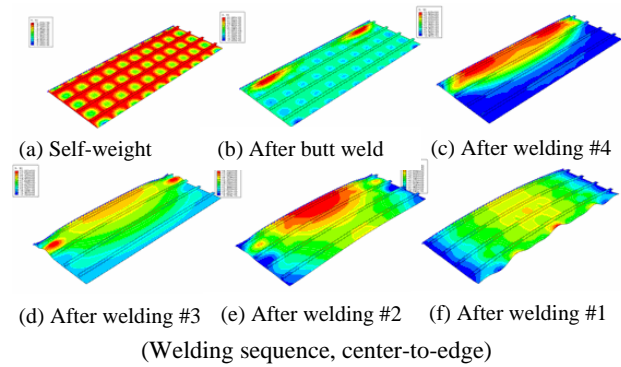


(a) Self-weight    (b) After butt weld    (c) After welding #4

(d) After welding #3    (e) After welding #2    (f) After welding #1

(Welding sequence, center-to-edge)

**Fig. 22. Deformed Shapes After Welding Each Stiffener**

Considering results of these two welding sequences, it is expected that a nonsymmetrical buckling distortion would be observed if this panel were welded from one edge to the other edge; edge to center, and then center to edge; the edge at start (edge to center sequence) would have more severe buckling distortion than the edge at end (center to edge sequence). Fig.23 shows the measured nonsymmetrical buckling distortion after welding. It is, therefore, beneficial to adopt the center to edge sequence on both sides to reduce buckling propensity in this type of panel.
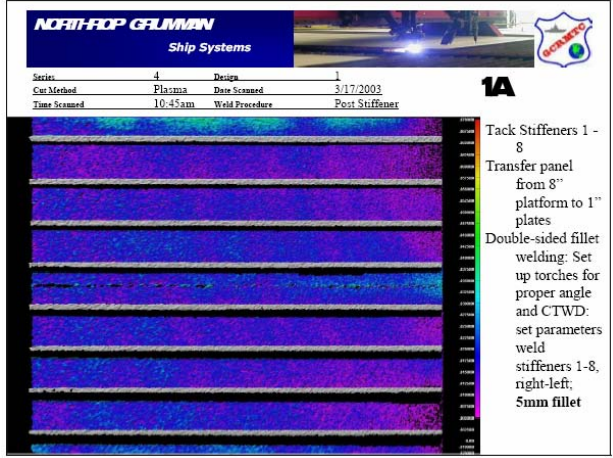


**Fig. 23 LIDAR Scan for NGSS Panel Design #1 without TTT**

## CONCLUSIONS

The applicability of Q-WELD™ in buckling analysis was evaluated via comparison with the results of a series of physical test panels. Eigenvalue and elastic-large deformation analyses were performed to evaluate the buckling propensity of each tested panel with and without TTT.

The Q-WELD™ predicted buckling propensity was in good agreement with all physical test results. The following conclusions can be drawn based on the analysis results:

- TTT effectively increases buckling resistance of all tested panels.

- The complex panel with inserts (Case 3) has higher buckling propensity than the simple panel (Case 2); buckling resistance of the complex panel with inserts would be decreased by the geometric imperfections resulting from cutting, fitting and insert welding.

- Buckling depends on welding sequences; it is recommend welding starts from the regions with higher buckling resistance to minimize the geometric imperfections for the subsequent welding.

- Buckling of panels can be reduced by using the center to edge welding instead of the edge to edge welding.

- Efficiency of TTT depends on the distance between welding and TTT; TTT should be away from welding to avoid material degradation, change of plastic strains; lateral tensioning induced by TTT on the free edges may be one of sources increasing the buckling resistance with increase of the distance between welding and TTT.

## ACKNOWLEDGEMENTS

## REFERENCES

ABAQUS User's Manual. *HKS* Co. USA.(2004)

CARLSON, C.A. "1979 A Parametric Study of Collapse of Stiffened Plates in Compression." *The Structural Engineer*, Vol.2 (1979)

GUAN, Q. LEGGATT, R.H., and BROWN, K.W., "1988 Low Stress, non-distortion (LSND) TIG welding of thin-walled structural elements." *The welding Institute Research Report 374*, Abington, Cambridge, U.K.

HORNE, M.R and NARAYANAN, R. "1977 Ultimate Strength of Stiffened Panels under Uniaxial Compression." *Steel Plated Structures*, Crosby Lockwood Staples, London: 1-23.

HORNE, M.R and NARAYANAN, R. "1976 The Strength of Straightened Welded Steel Stiffened Plates." *The Struct. Eng.*, Vol.54A(1976): 437-443

HUANG, T.D., DONG, P., DECAN, L.A. and HARWIG, D.D., "2003 Residual Stresses and Distortions in Lightweight Ship Panel Structures", *Technology Review Journal*, Spring/Summer (2003)

HUANG, T.D., DECAN, L.A., HARWIG, D.D., DONG, P., MOHR, B. KUMAR, R., "2004 Shipboard Applications of Lightweight Structures", *Gulf Coast Region Maritime Technology Center (GCRMTC) Report*, Project No. 327-02-5137 (2004)

HUANG, T.D., HARWIG, D.D., DONG, P., and DECAN, L.A. , "2005 Engineering and Ship Production Technology for Lightweight Structures", *Technology Review Journal*, Spring/Summer (2005)

JUNG, G.H. "2003 Plasticity-Based Distortion Analysis for Fillet Welded Thin Plate T-Joints." *Ph.D. Dissertation*, The Ohio State University, Columbus, Ohio. USA (2003).

JUNG, G.H. and TSAI, C.L. "2004 Plasticity-Based Distortion Analysis for Fillet Welded Thin-Plate T-Joints." *Welding Journal*, 87(6) (2004):177s-187s.

JUNG, G.H. and TSAI, C.L. "2004 Fundamental Studies on the Effect of Distortion Control Plans on Angular Distortion in Fillet Welded T-Joints." *Welding Journal*, 87(7) (2004):213s-223s.

JUNG, G.H., "2005 The prediction of welding distortions using shell element-based elastic analysis, Q-WELD™." Materials Science & Technology 2005.

JUNG, G.H. and YANG, Y.P., "2005 Practices of predicting welding-induced distortions using Q-WELD™." 2005 ABAQUS Central Users' Conference

MICHALERIS, P. and SUN, X., "1997 Finite Element Analysis of Thermal Tensioning Techniques Mitigating Weld Buckling Distortion.", *Welding Journal*, 76(11):451s-457s

SMITH, C.S. and KIRKWOOD, W. "1977 Influence of Initial Deformation and Residual Stresses in Inelastic Flexural Buckling of Stiffened Plates and Shells." *Steel Plated Structures*, Crosby Lockwood Staples, London: 838-864